ЖЭТФ, 2015, том 148, вып. 6 (12), стр. 1130–1136

GRAVITATING HOPFIONS

Ya. M. Shnir *

Joint Institute for Nuclear Research
141980, Dubna, Moscow Region, Russia

Received May 30, 2015

We construct solutions of the $3+1$ dimensional Faddeev–Skyrme model coupled to Einstein gravity. The solutions are static and asymptotically flat. They are characterized by a topological Hopf number. We investigate the dependence of the ADM masses of gravitating Hopfions on the gravitational coupling. When gravity is coupled to flat space solutions, a branch of gravitating Hopfion solutions arises and merges at a maximal value of the coupling constant with a second branch of solutions. This upper branch has no flat space limit. Instead, in the limit of a vanishing coupling constant, it connects to either the Bartnik–McKinnon or a generalized Bartnik–McKinnon solution. We further find that in the strong-coupling limit, there is no difference between the gravitating solitons of the Skyrme model and the Faddeev–Skyrme model.

DOI: 10.7868/S0044451015120081

1. INTRODUCTION

There are many nonlinear classical field theories in flat spacetime that admit topologically stable soliton solutions. These are particle-like, globally regular localized field configurations with finite energy. Interesting examples in $d = 3+1$ dimensions are the original Skyrme model [1] and the Faddeev–Skyrme model [2]. The Skyrme model is a nonlinear scalar $O(4)$ sigma model; under certain assumptions it can be derived by expanding a low-energy effective Lagrangian in the large-N_c limit [3], with the topological charge of the multisoliton configuration set in correspondence with the physical baryon number. The Faddeev–Skyrme model is a modified $O(3)$ sigma model, and hence the topological properties of the corresponding solitons, so-called Hopfions, are quite different from those of Skyrme-model solutions: the Hopfions are string-like configurations classified by the linking number, the first Hopf map $S^3 \to S^2$ [4–6].

The structure of both models looks similar: the corresponding Lagrangian includes the usual sigma-model term, the Skyrme term, which is quartic in derivatives of the field, and a potential term that does not contain derivatives. Recently, some modifications of both models were proposed to approach the topological bound [7, 8] preserving topological properties of the corresponding solitons.

When gravity is coupled to the Skyrme model, this has a significant effect on the solutions. It turns out that there are hairy black hole solutions of the Einstein–Skyrme theory [9–11]. Historically, that was the first example of constructions of hairy black holes. These solutions are stable, asymptotically flat, and have a regular horizon; furthermore, they can be viewed as bound states of Skyrmions and Schwarzschild black holes [12]. Axially symmetric static solutions of the Einstein–Skyrme model with topological charge two were studied in [13]. Recently, in [14], self-gravitating BPS Skyrmions were used in describing bulk properties of neutron stars.

The globally regular gravitating Skyrmions in an asymptotically flat space were studied in [10, 11]. It was shown that there are two branches of solutions, one of which emerges smoothly from the flat space Skyrmion configuration. As the effective gravitational coupling constant is increased from zero, this branch terminates at some critical value of the coupling, beyond which gravity becomes too strong for self-gravitating Skyrmions to persist. There, it merges with a second branch, which extends all the way back to the vanishing coupling constant. Along this branch, the mass of the gravitating Skyrmion rapidly increases and the solution becomes unstable. Surprisingly, it was shown in [11] that in the limit of vanishing coupling, the gravitating Skyrmion approaches

*E-mail: shnir@theor.jinr.ru

the lowest Bartnik–McKinnon (BM) solution of the SU(2) Einstein–Yang–Mills theory [15]. This pattern is rather similar to the branch structure of gravitating monopole–antimonopole chains and vortex rings in Einstein–Yang–Mills–Higgs theory [16, 17], although the reason for its existence is different.

The properties of gravitating Skyrmions were considered in many works, for example, configurations with discrete symmetry were investigated in [18] and spinning gravitating Skyrmions were studied in [19]. Modifications of the Einstein–Skyrme model with cosmological constant were investigated in [20, 21]. However, to the best of our knowledge, the analysis of properties of gravitating solitons of the Einstein–Faddeev–Skyrme system has not yet been done, although the Hopfions in flat space have been intensively studied over recent years [4–6].

In this paper, we construct globally regular gravitating Hopfions. Because the consistent consideration of solitons with higher Hopf charges is related to the complicated task of full numerical simulations in 3D [6], we restrict ourself to the case of static Hopfions of degrees $Q \le 4$. Using the rational map parameterization of the scalar field, we produce an initial configuration of a given degree, to be used as an input file in our numerical scheme. We study the corresponding field configurations in the Einstein–Faddeev–Skyrme model numerically. We show that the general pattern of evolution of the configuration is very similar to the branch structure of the Einstein–Skyrme system that links the flat space Skyrmions and the BM solution.

2. THE MODEL

The Einstein–Faddeev–Skyrme model in asymptotically flat 3+1 dimensional space is defined by the action

$$S = \frac{1}{32\pi^2} \int \left\{ \frac{2\pi R}{G} - \left[e^2 (\partial_\mu \Phi^a \partial^\mu \Phi^a) + \frac{1}{4\kappa^2} F_{\mu\nu} F^{\mu\nu} + V[\Phi] \right] \right\} \times \sqrt{-g} d^4x, \quad (1)$$

where the gravity part of the action is the usual Einstein–Hilbert action with the curvature scalar R, g denotes the determinant of the metric, G and M are the gravitational constant and the mass of the Faddeev–Skyrme field, and e and κ are the Hopfion coupling constants. We note that in the natural units in which $c = \hbar = 1$, the parameter e^2 has the dimension $[e^2] = [ml^{-1}] = \mathrm{MeV}^2$ while the constant $[\kappa^2] = [m^{-1} l^{-1}]$ is dimensionless.

We next define

$$F_{\mu\nu} = \varepsilon_{abc} \Phi^a \partial_\mu \Phi^b \partial_\nu \Phi^c,$$

which is the pullback of the area form on the target space S^2. An additional potential term $V[\Phi] = M^2[1 - (\Phi_3)^2]$ breaks down the global SO(3) symmetry of the model. We note that this term is optional: the existence of static soliton solutions of model (1) is allowed by the Derrick theorem even if the mass parameter $M = 0$. However, this term is necessary in order to stabilize the isospinning Hopfions [22, 23].

The triplet of the real scalar field components $\Phi^a = (\Phi_1, \Phi_2, \Phi_3)$ is restricted to the unit sphere, $\Phi^a \cdot \Phi^a = 1$, and hence the field is a map $\Phi : \mathbb{R}^3 \to S^2$. A topological restriction on the field ϕ^a is that it approaches its vacuum value at the spacial boundary, $\Phi \to (0, 0, 1)$ as $r \to \infty$, and therefore the one-point compactification of the domain space $\mathbb{R}^3$ to S^3 defines static finite-energy solutions of the model as the first Hopf map $\Phi : \mathbb{S}^3 \to S^2$ that belongs to an equivalence class characterized by the third homotopy group $\pi_3(S^2) = \mathbb{Z}$. Explicitly, the integer-valued Hopf invariant is defined nonlocally as

$$Q = \frac{1}{16\pi^2} \int\limits_{\mathbb{R}^3} \varepsilon_{ijk} \mathcal{F}_{ij} \mathcal{A}_k, \quad (2)$$

where the one-form $\mathcal{A} = \mathcal{A}_k dx^k$ is defined via $\mathcal{F} = d\mathcal{A}$, i. e., the two-form $\mathcal{F}$ is closed, $d\mathcal{F} = 0$. Invariant (2) can be interpreted geometrically as the linking number of two loops obtained as the preimages of any two generic distinct points on the target space S^2.

Similarly to the case of the Einstein–Skyrme model [11], we can rescale the model by introducing the dimensionless radial coordinate $x = e\kappa r$, the gravitational coupling constant $\alpha^2 = Ge^2/2\pi$, and the rescaled mass parameter $\hat{M} = M/e^2\kappa$. Then action (1) becomes

$$S = \frac{e}{32\kappa\pi^2} \int \left\{ \frac{R}{\alpha^2} - \left(\partial_\mu \Phi^a \partial^\mu \Phi^a + \frac{1}{4} F_{\mu\nu} F^{\mu\nu} + \hat{M}^2 (1 - (\Phi_3)^2) \right) \right\} \times \sqrt{-g}\, d^4x. \quad (3)$$

To obtain gravitating static axially symmetric solutions, we use the usual Lewis–Papapetrou metric in isotropic coordinates:

$$ds^2 = -f dt^2 + \frac{m}{f} dr^2 + \frac{mr^2}{f} d\theta^2 + \frac{lr^2 \sin^2\theta}{f} d\varphi^2, \quad (4)$$

where the metric functions f, m, and l are functions of the radial variable r and the polar angle θ only. The z axis ($\theta = 0, \pi$) represents the symmetry axis.

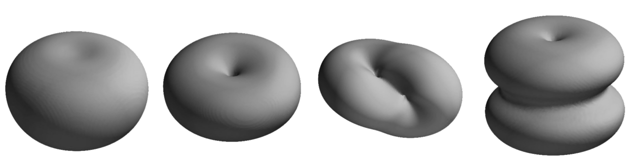

Fig. 1. Energy density isosurfaces of the Hopfions of degrees 1 to 4 (from left to right)

For the lowest values of the corresponding Hopf charge $Q = 1, 2$, the simplest soliton solutions can be constructed using the axially symmetric ansatz [4] written in terms of the functions $X = X(r,\theta), Y = Y(r,\theta)$, and $Z = Z(r,\theta)$:

$$\Phi_1 + i\Phi_2 = F(r,\theta)e^{i(m\Psi(r,\theta)+n\varphi)} \equiv \equiv [X(r,\theta) + iY(r,\theta)]e^{in\varphi},$$

$$\Phi_3 = Z(r,\theta),$$

where $n, m \in \mathbb{Z}$.

An axially symmetric configuration of the matter field of this type is commonly referred to as $\mathcal{A}_{m,n}$, where the first subscript corresponds to the number of twists along the loop and the second label is the usual $O(3)$ sigma-model winding number associated with the map $S^2 \to S^2$. The Hopf invariant of this configuration is $Q = mn$.

However, for higher-degree Hopfions, twisted, knotted, and linked configurations occur [5, 6], and furthermore, the number of local energy minima configurations grows with Q. Here we consider the twisted configuration $\widetilde{\mathcal{A}}_{3,1}$ of degree 3 and the $\mathcal{A}_{2,2}$ axially symmetric solution of degree 4. The latter configuration, which is a global minimum in this sector, may be thought of as two adjacent Hopfions $\mathcal{A}_{2,1}$. The energy isosurfaces of these flat-space configurations are shown in Fig. 1.

Using the rational map projection from the sphere $S^3 \subset \mathbb{C}^2$ onto the complex projective line $\mathbb{CP}^1$ [6], we can parameterize the initial configuration as

$$W = \frac{\Phi_1 + i\Phi_2}{1+\Phi_3} \equiv \frac{Z_1^\alpha Z_0^\beta}{Z_1^a + Z_0^b}, \qquad (5)$$

where

$$(Z_1, Z_0) = = \left((x+iy)\frac{\sin h(r)}{r}, \cos h(r) + iz\frac{\sin h(r)}{r}\right) \qquad (6)$$

and $h(r)$ is some monotonic function of the radial variable $r = \sqrt{x^2+y^2+z^2}$ with the boundary conditions $h(0) = \pi$ and $h(\infty) = 0$. Such a map has the degree $Q = \alpha\beta + ab$, and it therefore allows us to construct an initial configuration of any degree.

A peculiar feature of the Faddeev–Skyrme model is that for a given degree Q, there are usually several different stable static soliton solutions of rather similar energy. In particular, there are two solutions in the sector of degree three, $\tilde{\mathcal{A}}_{3,1}$ and an axially symmetric configuration $\mathcal{A}_{3,1}$. The energy of the latter soliton is slightly higher, but the inclusion of the mass term and/or excitation of the isorotational degrees of freedom may change the situation [23]. Hereafter, we restrict our consideration to the axially symmetric solutions of degrees $Q \le 4$.

The complete set of field equations that follow from the variation of the action of Einstein–Faddeev–Skyrme model (1) can be solved when we impose the boundary conditions and use the parameterization of the metric in (4). Then the field equations reduce to a set of six coupled partial differential equations, to be solved numerically.

As usual, they follow from the regularity on the symmetry axis and symmetry requirements as well as the condition for the energy to be finite. In particular, we have to take into account that the asymptotic value of the Hopfion field is restricted to the unit sphere and the metric functions must approach unity at the spacial boundary. Explicitly, we impose the conditions

$$\begin{gathered} \Phi_1\Big|_{r\to\infty} \to 0\,, \quad \Phi_2\Big|_{r\to\infty} \to 0\,, \quad \Phi_3\Big|_{r\to\infty} \to 1, \\ f\Big|_{r\to\infty} \to 1, \quad m\Big|_{r\to\infty} \to 1, \quad l\Big|_{r\to\infty} \to 1 \end{gathered} \qquad (7)$$

at infinity and

$$\begin{gathered} \Phi_1\Big|_{r\to 0} \to 0\,, \quad \Phi_2\Big|_{r\to 0} \to 0\,, \quad \Phi_3\Big|_{r\to 0} \to 1, \\ \partial_r f\Big|_{r\to 0} \to 0\,, \quad \partial_r m\Big|_{r\to 0} \to 0\,, \quad \partial_r l\Big|_{r\to 0} \to 0 \end{gathered} \qquad (8)$$

at the origin.

The regularity condition for the functions on the symmetry axis yields

$$\begin{gathered} \Phi_1\Big|_{\theta\to 0,\pi} \to 0\,, \quad \Phi_2\Big|_{\theta\to 0,\pi} \to 0\,, \quad \Phi_3\Big|_{\theta\to 0,\pi} \to 1, \\ \partial_\theta f\Big|_{\theta\to 0,\pi} \to 0\,, \quad \partial_\theta m\Big|_{\theta\to 0,\pi} \to 0\,, \quad \partial_\theta l\Big|_{\theta\to 0,\pi} \to 0. \end{gathered} \qquad (9)$$

To satisfy the regularity condition $m(r,0) = l(r,0)$, we introduce the auxiliary function

$$g(r,\theta) = l(r,\theta)/m(r,\theta)$$

with the boundary conditions

$$g(0,\theta) = g(\infty,\theta) = g(r,0) = 1; \quad \partial_\theta g(r,\pi/2) = 0.$$

We check this condition as a test for correctness of our numerical results.

3. NUMERICAL RESULTS

The numerical calculations are mainly performed on an equidistant grid in spherical coordinates r and θ, using the compact radial coordinate $x = r/(1+r) \in [0:1]$ and $\theta \in [0,\pi]$. To find solutions of the Euler–Lagrange equations that follow from rescaled action (3) and depend parametrically on the effective gravity constant α, we used the software package CADSOL based on the Newton–Raphson algorithm [24]. This code solves a given system of nonlinear partial differential equations subject to a set of boundary conditions on a rectangular domain. Typical grids we used have sizes 90×70. The resulting system is solved iteratively until convergence is achieved.

Apart from some initial guess for the solution, CADSOL also requires the Jacobian matrices for the equations with respect to the unknown functions and their first and second derivatives, and the boundary conditions. This software package also provides error estimates for each function, which allows judging the quality of the computed solution. The relative errors of the solutions we found are of the order 10^{-4} or smaller. We also introduce an additional Lagrangian multiplier to constrain the field to the surface of a unit sphere and fix the value of the mass parameter $M = 1$.

We note that the dimensionless gravitational coupling constant $\alpha^2 = Ge^2/2\pi$ vanishes if (i) the Newton constant $G \to 0$, or, (ii) $e \to 0$. In the former case, we recover the usual solitons of the Faddeev–Skyrme model in flat space, and in the second case, the Dirichlet term in action (1) vanishes. Thus, similarly to the case of self-gravitating monopole–antimonopole systems in the asymptotically flat Einstein–Yang–Mills–Higgs theory [16, 17], Yang–Mills sphalerons in the AdS_4 spacetime [25], and solitons of the Einstein–Skyrme model [11, 26], we expect that there are two branches of solutions of the Einstein–Faddeev–Skyrme model.

We have found numerical evidence that when gravity is coupled to the Faddeev–Skyrme model, a branch of gravitating Hopfions emerges from the flat-space Hopfion solution and extends to a maximal value α_{cr} where it merges with the upper mass branch. Indeed, as the gravitational coupling constant increases, the background becomes more and more deformed and, at some critical value of the coupling, gravity becomes too strong for solutions to persist. The critical value α_{cr} at which a backbending is observed slightly decreases as the topological charge of the Hopfion inscreases (cf. Figs. 2 and 3).

Parameterization (4) allows us to find the dimensionless ADM mass of the configuration μ, defined by the value of the derivative of the metric function f at the boundary:

$$\mu = \frac{1}{2\alpha^2} \lim_{x\to\infty} \partial_x f. \tag{10}$$

To perform another check of our numerics for correctness, we compare this value with the results of direct evaluation of the integral over the T_{00} component of the total energy–momentum tensor of matter and gravity.

Along the first (lower) branch, the mass of the gravitating Hopfions decreases with increasing α, since the attraction in the system increases with increasing the gravitational strength. Along the second (upper) branch, by contrast, mass (10) increases strongly with decreasing the coupling α, and the solutions shrink correspondingly. In the limit of a vanishing coupling constant, the mass μ then diverges and the solutions shrink to zero size. We illustrate this pattern in Fig. 2. Also, the gravitational interaction along this branch remains strong. In Fig. 3, we exhibit the value of the metric functions f and l at the origin for configurations of degrees 1 to 4; both functions remains finite in this limit.

This pattern is similar to the well-known picture of the evolution of self-gravitating skyrmions [9–11, 19] and monopole–antiminopole pairs [16, 17], which on the upper unstable branch are linked to the spherically symmetric Bartnik–McKinnon limit solution [15].

In the case of self-gravitating Hopfions, the structure of the $e^2 \to 0$ limit solution can be better understood when we introduce the rescaled radial coordinate $\hat{x} = x/\alpha$ and the rescaled mass $\hat{\mu} = \alpha\mu$ [11]. We then observe that the rescaled mass remains finite in the limit $\alpha \to 0$, as shown in Fig. 2*b*. Furthermore, the value of the limit mass is approaching the mass of the corresponding generalized Bartnik–McKinnon solution [27]. Indeed, in the limit $e \to 0$, the remaining Skyrme term in action (1) has a structure that is identical to the Yang–Mills theory action expressed in terms of the field strength tensor $F_{\mu\nu}$.

We note that a similar truncated Faddeev–Skyrme model without the Dirichlet term was recently considered on the space $\mathbb{S}^3 \times \mathbb{R}$ [8]. It turns out that it supports the existence of compacton solutions that saturate the topological bound. These configurations are

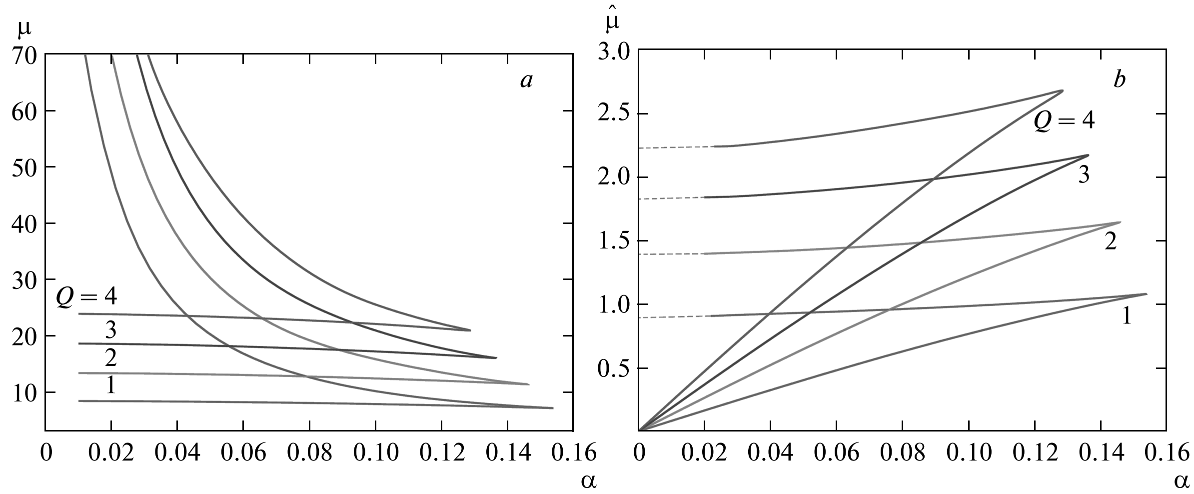

Fig. 2. The mass μ (a) and the scaled mass $\hat{\mu}$ (b) of the gravitating Hopfions of degrees 1 through 4 are shown as functions of the coupling constant α at $M = 1$. The dotted lines extend the Hopfion curves of the scaled mass to the mass of the corresponding generalized Bartnik–McKinnon solution

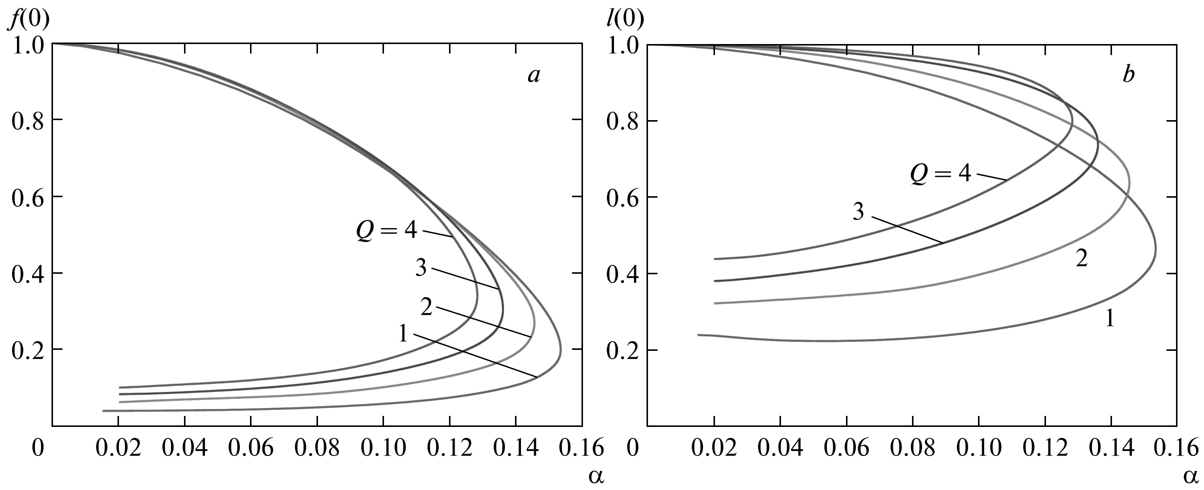

Fig. 3. The values of the metric functions $f(0)$ (a) and $l(0)$ (b) of the gravitating Hopfions of degrees 1 through 4 at the origin are shown as functions of the gravitational coupling constant α at $M = 1$

different from the vacuum only on some finite domain of the coordinate space. Furthermore, this model is integrable. Thus, these compactons can be regarded as an approximation to the strongly gravitating Hopfions in the limit $\alpha \to 0$.

To clarify this observation, in Fig. 4a, we plot the metric function f of the upper branch $\mathcal{A}_{1,1}$ solution at $\alpha^2 = 0.0004$ and the corresponding field component Φ^3 in the coordinates $\log r$, θ. Clearly, we can identify three distinct regions. In the first region, as can be seen in Fig. 4 the metric function f remains very small but constant without any angular dependence. The corresponding matter fields of the Hopfion are approximately trivial in this inner region. In the second transition region, the metric varies up to the maximum value $f = 1$; this is a small region where the energy of the matter field is located. In Fig. 5, we presented the surfaces of constant energy density of the gravitating $\mathcal{A}_{1,1}$ and $\mathcal{A}_{2,1}$ Hopfions. For the $Q = 1$ Hopfion, the energy density exhibits a structure of a pumpkin-shaped sphere with a maximum at the origin, and for $Q = 2$, the configuration it is a deformed sphere surrounded by a torus-like ring (cf. the corresponding flat-space configurations in Fig. 1). Finally, in the third outer re-

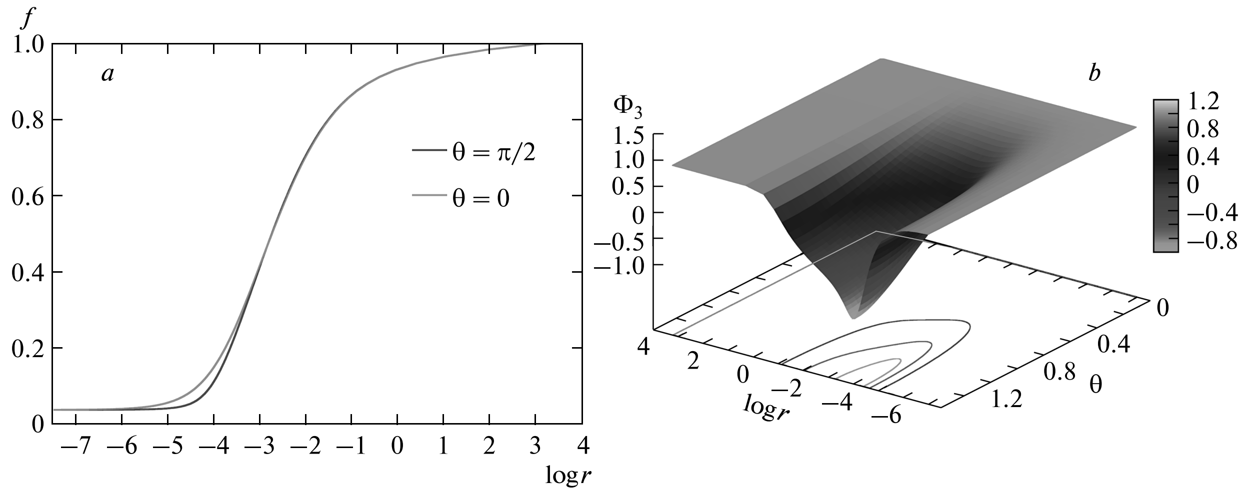

Fig. 4. The metric function $f(r,\theta)$ (a) and the third component of the field of the gravitating Hopfion of degree 1 on the upper branch (b) are shown in the logarithmic radial coordinate $\log r$ at $\alpha^2 = 0.0004$ at $M = 1$

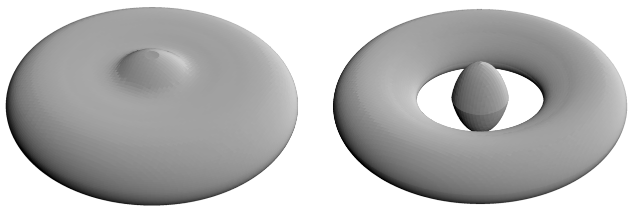

Fig. 5. The isosurfaces of the energy density ($\epsilon = 4\cdot 10^6$) of the gravitating axially symmetric Hopfions of degrees 1 and 2 on the upper branch are shown at $\alpha^2 = 0.0004$ and $M = 1$. The characteristic size of the configurations is about $r_{core} \sim 0.8$ in the rescaled radial coordinate $\tilde{r} = \alpha r$

gion, the metric functions are approaching the flat-space limit values while the components of the Hopfion field are approximately in the vacuum. Clearly, this pattern agrees with the corresponding behavior of the Bartnik–McKinnon solutions [15, 26] and the regular solutions of the Einstein–Skyrme model [11]. Hence, this behavior is generic, being independent of the topological properties of the matter field.

4. CONCLUSIONS

The main purpose of this paper was to present new type of self-gravitating solitons in the Einstein–Faddeev–Skyrme theory. We have focused on the configurations of lower degrees up to $Q = 4$. These solutions are asymptotically flat and globally regular.

As regards the dependence of the gravitating Hopfions on the gravity coupling constant, we observe the same general pattern as for solitons of the Einstein–Skyrme model and the sphaleron solutions of the Einstein–Yang–Mills–Higgs theory. In all these cases, a lower branch of gravitating solitons emerges from the corresponding flat-space configurations, and merges with the upper branch at a maximal value of the gravitational coupling. The upper branch extends back to the limit $\alpha \to 0$, where solutions approach the corresponding (generalized) Bartnik–McKinnon solutions of the SU(2) Einstein–Yang–Mills theory. Hence, we can conclude that the topological characteristics of the matter field do not affect the limit behavior of gravitating solitons.

One question we did not address concerns the stability of the gravitating Hopfions. However, it is known that the solitons of the Einstein–Skyrme model are stable on the lower branch and are unstable on the upper branch, and there is a reason to believe that the gravitating Hopfions on the upper branch are also unstable.

There are various possible extensions of the solutions discussed in this paper. First, our preliminary results indicate the existence of static axially symmetric black hole solutions with Hopfion hair. But constructing gravitating Hopfion solutions of higher degrees currently remains a numerical challenge. It would also be interesting to address the question of how inclusions of a cosmological constant affect the properties of a gravitating Hopfion.

We thank P. Bizon, J. Kunz, E. Radu, and M. Volkov for the useful discussions and valuable comments. We gratefully acknowledge support from the A. von Humboldt Foundation in the framework of the Institutes Linkage Program.

REFERENCES

1. T. H. R. Skyrme, Proc. Roy. Soc. London A **260**, 127 (1961).

2. L. D. Faddeev, Princeton preprint IAS-75-QS70 (1975); L. D Faddeev and A. Niemi, Nature **387**, 58 (1997); Phys. Rev. Lett. **82**, 1624 (1999).

3. E. Witten, Nucl. Phys. B **223**, 422 (1983); *ibid* **223**, 433 (1983).

4. J. Gladikowski and M. Hellmund, Phys. Rev. D **56**, 5194 (1997).

5. R. Battye and P. Sutcliffe, Phys. Rev. Lett. **81**, 4798 (1998).

6. P. Sutcliffe, Proc. Roy. Soc. London A **463**, 3001 (2007).

7. C. Adam, J. Sanchez-Guillen, and A. Wereszczynski, Phys. Rev. D **82**, 085015 (2010).

8. C. Adam, J. Sanchez-Guillen, and A. Wereszczynski, J. Phys. A **43**, 345402 (2010).

9. H. Luckock and I. Moss, Phys. Lett. B **176**, 341 (1986).

10. S. Droz, M. Heusler, and N. Straumann, Phys. Lett. B **268**, 371 (1991).

11. P. Bizon and T. Chmaj, Phys. Lett. B **297**, 55 (1992).

12. A. Ashtekar, A. Corichi, and D. Sudarsky, Class. Quant. Grav. **18**, 919 (2001).

13. N. Sawado, N. Shiiki, K. I. Maeda, and T. Torii, Gen. Rel. Grav. **36**, 1361 (2004).

14. C. Adam, C. Naya, J. Sanchez-Guillen, R. Vazquez, and A. Wereszczynski, Phys. Lett. B **742**, 136 (2015).

15. R. Bartnik and J. Mckinnon, Phys. Rev. Lett. **61**, 141 (1988).

16. B. Kleihaus and J. Kunz, Phys. Rev. Lett. **85**, 2430 (2000).

17. B. Kleihaus, J. Kunz, and Y. Shnir, Phys. Rev. D **71**, 024013 (2005).

18. T. Ioannidou, B. Kleihaus, and J. Kunz, Phys. Lett. B **635**, 161 (2006).

19. T. Ioannidou, B. Kleihaus, and J. Kunz, Phys. Lett. B **643**, 213 (2006).

20. N. Shiiki and N. Sawado, Phys. Rev. D **71**, 104031 (2005).

21. Y. Brihaye and T. Delsate, Mod. Phys. Lett. A **21**, 2043 (2006).

22. R. Battye and M. Haberichter, Phys. Rev. D **87**, 105003 (2013).

23. D. Harland, J. Jäykkä, Ya. Shnir, and M. Speight, J. Phys. A **46**, 225402 (2013).

24. W. Schönauer and R. Weiß, J. Comput. Appl. Math. **27**, 279 (1989); M. Schauder, R. Weiß, and W. Schönauer, The CADSOL Program Package, Univ. Karlsruhe (1992). Interner Bericht Nr. 46/92.

25. O. Kichakova, J. Kunz, E. Radu, and Y. Shnir, Phys. Rev. D **90**, 124012 (2014).

26. M. S. Volkov and D. V. Galtsov, Pisma v Zh. Eksp. Teor. Fiz. **50**, 312 (1989) [JETP Lett. **50**, 346 (1989)].

27. R. Ibadov, B. Kleihaus, J. Kunz, and Y. Shnir, Phys. Lett. B **609**, 150 (2005).